Microscopic Calculation of Superfluidity and Kinetic Energies in Isotopic Liquid Helium Mixtures

Massimo Boninsegni[1] and Saverio Moroni[2]
[1]*Department of Physics and Astronomy, University of Delaware, Newark, Delaware 19716*
[2]*International Centre for Theoretical Physics, Trieste, Italy*
(Received 10 October 1996)

The superfluid transition in homogeneous liquid ^{3}He-^{4}He mixtures is studied numerically by restricted path integral Monte Carlo simulations. Finite-size scaling analysis of the results for the superfluid fraction yields values of the critical ^{3}He concentration in quantitative agreement with experiment. The calculated single-particle kinetic energies of the two isotopes feature a clear, monotonic dependence on the ^{3}He concentration. [S0031-9007(97)02584-2]

PACS numbers: 67.60.g, 61.20.Ja

The investigation of the phase diagram of isotopic liquid helium mixtures has motivated a considerable amount of theoretical [1] and experimental [2] work in the course of a few decades. In recent times, the experimental effort has been primarily devoted to the study of dynamic properties of the mixtures, such as superfluidity, particularly in confined geometries [3], as well as the momentum distribution [4,5]. The aim is to gain understanding on the effect of impurities on superfluidity, as well as to study a Fermi liquid (^{3}He) whose degeneracy can be "tuned" by varying its concentration χ. On the theoretical side, various types of microscopic calculations, based on realistic interatomic potentials, have yielded important insight in the energetic and structural properties of the mixtures [6]; however, no microscopic study of superfluidity in the homogeneous mixture has yet been reported.

Numerical simulations based on the path integral Monte Carlo (PIMC) method afford a remarkably accurate quantitative description of the superfluid transition in pure liquid ^{4}He [7,8]; although the calculations are demanding and a statistical accuracy of better than a few percent for the superfluid density is hard to achieve, it is possible to determine reliably the transition temperature by performing finite-size scaling analysis [9]. The application of path integrals to isotopic liquid helium mixtures is relatively recent [10], following the introduction of the restricted path integral Monte Carlo (RPIMC) technique, which effectively overcomes the well-known *sign* problem, thereby allowing the simulation of Fermi systems, such as ^{3}He [11]. In Ref. [10] the suitability of RPIMC to explore intriguing aspects of the phase diagram of the mixture at low temperature, such as the separation into two distinct phases, was demonstrated.

In this work we extend the investigation carried out in Ref. [10] by calculating the ^{4}He superfluid fraction $\rho_s(\chi, T)$ and the kinetic energies $K_3(\chi, T)$ and $K_4(\chi, T)$ of the two isotopes in a temperature range ($1 \leq T \leq 2$ K) where the mixture is homogeneous; i.e., no phase separation occurs. This region of the phase diagram has been extensively probed experimentally [2]; thus, a comparison with accurate measurements is possible, thereby gauging the effectiveness of PIMC to study, for example, superfluidity of helium mixtures in confined geometries, as well as of "dirty" Bose systems or other mixtures of Bose and Fermi components, a problem of potential impact in different areas of physics.

The ^{3}He quasiparticle gas in the mixture in equilibrium is a normal Fermi liquid with a degeneracy temperature from $\sim$0.5 K at $\chi \sim 0.1$ to around 1.5 K at $\chi \sim 0.6$; thus, effects of Fermi statistics are not entirely negligible in the (χ,T) region of interest here; at lower temperatures, they influence considerably the physics of the mixtures, for example, causing a finite ^{3}He solubility in ^{4}He in the $T \longrightarrow 0$ limit, as observed in a PIMC simulation [10].

This Letter can be summarized as follows: we simulated a system of N helium particles in a cubic box with periodic boundary conditions. Of these particles, $n = \chi N$ are ^{3}He and the remaining $N - n$ ^{4}He atoms; only unpolarized mixtures were studied. The density of the system was set to the experimentally measured value corresponding to each (χ, T) pair considered [12]. We used an accepted two-body potential to model the interaction between helium atoms [13]. We computed $\rho_s(\chi, T)$ for systems with $N = 20$, 36, 54, and 108 particles. For all of these systems, our results show the expected decrease of $\rho_s(\chi, T)$ on increasing χ. As in any numerical study, the transition is smeared by finite-size effects; finite-size scaling analysis of our results shows consistency with the basic scaling hypothesis for pure liquid ^{4}He [9], and allows one to determine critical ^{3}He concentrations in quantitative agreement with experiment at the two temperatures considered. Single-particle kinetic energy estimates for the two isotopes at the temperatures and ^{3}He concentrations considered are in agreement with recent neutron scattering experimental data [5], as far as the ^{4}He component is concerned; $K_3(\chi, T)$, on the other hand, is significantly larger than in the experiment. Both $K_3(\chi, T)$ and $K_4(\chi, T)$ decreases monotonically with χ.

Before turning to a detailed presentation and discussion of our results, we briefly comment on the computational technique adopted in this work. Path integral Monte Carlo is a well-established numerical tool, allowing the computation of finite-temperature properties of quantum many-particle systems, including energetics, structural properties, and superfluid densities, directly from the microscopic Hamiltonian. Since excellent references exist where this method is thoroughly described [8], the details of PIMC will not be reviewed here. The restricted path integral Monte Carlo method is an extension of PIMC, capable of simulating Fermi systems without the well-known *sign* problem that prevents a straightforward application of any quantum Monte Carlo method to fermions. While PIMC is in principle numerically exact, RPIMC is in general only approximate; its accuracy depends on an initial guess for the nodal surface of the exact finite-temperature, many-body density matrix, which is adopted to "restrict" the many-particle paths through the configuration space [14]. In principle, exact results could be obtained if the true nodal surface were known; in practice, if the trial nodal surface is chosen appropriately, RPIMC yields accurate thermodynamics for Fermi systems.

The RPIMC procedure has been applied to the study of normal liquid ^{3}He [11], using the nodes of a free-particle density matrix, yielding accurate results at temperatures above 1 K. The same choice of nodal restriction was also adopted to study mixtures in Ref. [10], and in this work as well. Its use can be justified by the relatively low fermion densities in the (χ, T) regime considered here, in which ^{3}He should behave as an almost ideal Fermi gas. All technical details of the RPIMC calculations performed in this work are identical to those of Ref. [10]. In particular, the value of the imaginary time step [8] used in all the calculations performed in this work is $\tau = 0.025\ \mathrm{K}^{-1}$.

The "winding number" estimator [7,8] was adopted in this work to compute the superfluid fraction; it relates the superfluid signal to permutational exchange cycles involving a macroscopic number of ^{4}He atoms and spanning spatially the entire system [8]; for large system sizes, sampling these long cycles becomes increasingly inefficient, and, as a result, error bars are typically greater for larger systems. The presence of the nodal restriction entails no particular complication, but has the effect of slowing down considerably the convergence of the estimates, with respect to pure liquid ^{4}He. This is because the ^{4}He paths are affected by the ^{3}He nodes, and consequently diffuse less efficiently through configuration space, particularly at $\chi \geq 0.3$ and in systems with more than $N \sim 50$ particles. If we define a "pass" as an attempt to update a many-particle path, we performed typically of the order of 10^6 passes initially, to equilibrate the system, and 10^7 successively to calculate the averages.

Our results for $\rho_s(\chi, T)$ are shown in Fig. 1 for the two temperatures considered; in the figure, our results are compared to torsional oscillator measurements of $\rho_s(\chi, T)$ (Ref. [15]).

The values of $\rho_s(\chi, T)$ that we found at $\chi = 0$ (i.e., pure liquid ^{4}He) are consistent, within statistical uncertainties, with previous PIMC estimates [7,9]. As χ is increased, $\rho_s(\chi, T)$ decreases monotonically for all the systems studied, in qualitative agreement with experiment.

As expected, the χ-driven superfluid transition is smeared by finite-size effects, as clearly shown in Fig. 1, particularly at the higher of the two temperatures considered. The results approach the experimental values as the size of the system is increased; for example, within statistical errors the estimates obtained for $T = 1$ K on a 108-particle system are in agreement with experiment.

In order to characterize quantitatively the transition and provide meaningful estimates for experimentally measurable parameters, such as the critical concentration $\chi_c(T)$, i.e., the concentration at which $\rho_s(\chi_c, T) = 0$, finite-size scaling analysis of the results is needed. In pure liquid ^{4}He, $\rho_s(T) \sim t^{\nu}$, where $t = (T - T_c)/T_c$, in the vicinity of the critical temperature T_c.

The fundamental hypothesis of scaling [16] permits one to deduce a scaling relation for the superfluid fraction $\rho_s(L, t)$ for a finite system of size L

$$L^{\nu/\nu}\rho_s(L, t) \sim Q(L^{1/\nu}t), \tag{1}$$

where ν is the exponent associated to the divergence of the characteristic correlation length of the system in the vicinity of the phase transition, i.e., $\xi(t) \sim t^{-\nu}$. The function Q is unknown, but is analytic for a finite value of its argument, corresponding to a finite system.

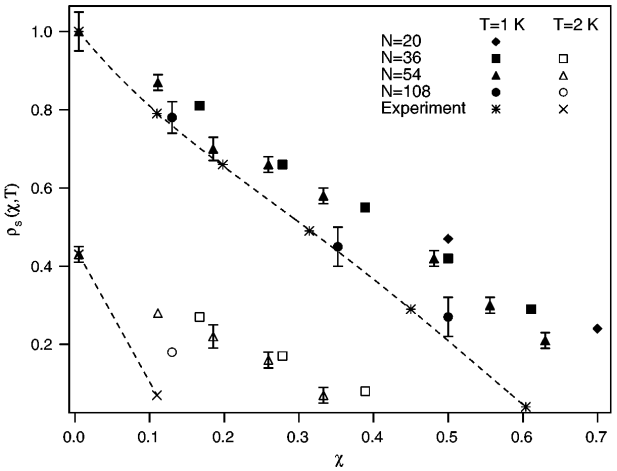

FIG. 1. Superfluid fraction $\rho_s(\chi, T)$ computed by RPIMC for a helium mixture at different ^{3}He concentrations χ and $T = 1$ (filled symbols) and $T = 2$ (open symbols) K. Stars and crosses refer to experimental results from Ref. [15]. When not shown, error bars are smaller than the size of the symbol. Dashed lines through experimental points are guides to the eye.

Finite-size scaling analysis of PIMC data for $\rho_s(L,t)$ in pure liquid ^{4}He has provided evidence that $\upsilon/\nu = 1$, consistently with more fundamental scaling arguments [9]. Experiments for mixtures have yielded so far evidence that ρ_s behaves in the vicinity of the critical temperature as in pure ^{4}He, though additional singular terms must be included to obtain an accurate fit to the data [2]; if one assumes this to be the case, the scaling relation (1) is then appropriate for a finite-size scaling analysis of PIMC data for $\rho_s(L,t)$ in the mixtures as well (note that the universal function Q does not depend on χ). According to Eq. (1), the functions $L^{\upsilon/\nu}\rho_s(L,\chi,t)$ for different values of L and for a given χ should all cross at $t = 0$, i.e., at $T = T_c(\chi)$; alternatively, for a given value of T they should all cross, as a function of χ, at the critical concentration χ_c at which $T = T_c(\chi_c)$.

Figure 2 shows the results for ρ_s scaled according to (1), with $\upsilon = \nu$. Within our statistical uncertainties, the data appear to conform to the scaling ansatz adopted. The curves cross at a critical concentration $\chi_c = 0.61 \pm 0.01$ at $T = 1$ K and $\chi_c = 0.11 \pm 0.01$ at $T = 2$ K. Both results are in excellent agreement with experiment [15]; this offers an *a posteriori* validation to the use of free-particle nodes for this problem. Note that, though our statistical errors do not allow one to draw a reliable conclusion on the value of υ/ν, χ_c is quite insensitive to it, analogously to what found for the critical temperature in pure liquid ^{4}He [9].

The path integral formalism offers a suggestive interpretation of superfluidity as due to the occurrence at low temperature of permutational exchange cycles involving a macroscopic fraction of all the ^{4}He atoms in the system [8]. The suppression of superfluidity observed on diluting ^{3}He in ^{4}He is simply due to the inhibiting effect that ^{3}He impurities have on these long permutations, owing to the repulsive hard core of the helium-helium interaction.

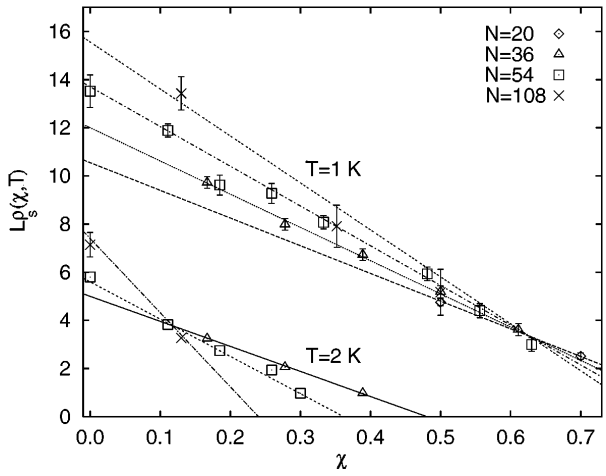

FIG. 2. Scaled superfluid fraction $L\rho_s(L,\chi,T)$ computed by RPIMC for a helium mixture at different ^{3}He concentrations χ and $T = 1$ (upper data set) and $T = 2$ (lower data set), for various system sizes. Lines are linear fits to the curves. When not shown, error bars are smaller than the symbol size.

Next we discuss our results for the kinetic energies of the two isotopes, $K_3(\chi,T)$ and $K_4(\chi,T)$, in the (χ,T) range explored. Experimentally, the value of the single-particle kinetic energy can be inferred from the second moment of the momentum distribution $n(p)$, probed by neutron scattering [17]. Values determined for the pure liquid isotopes are in basic agreement with various quantum Monte Carlo calculations [8,18].

For the mixtures, on the other hand, a disagreement between theory and experiment exists regarding the value of the kinetic energy of a single ^{3}He atom in liquid ^{4}He in the $T \longrightarrow 0$ limit. Analysis of neutron scattering measurements has yielded [4] an estimate of 11 ± 3 K, i.e., the same value as in pure liquid ^{3}He, within statistical uncertainties; however, a PIMC simulation [10] has yielded a larger value, namely 17.1 ± 0.1 K, in substantial quantitative agreement with previous theoretical estimates [6]. This kinetic energy enhancement arises from the greater localization experienced by a single ^{3}He atom in liquid ^{4}He than in pure liquid ^{3}He, due to the lower local density in the latter [10]. By the same token, the kinetic energy of a single ^{4}He atom in liquid ^{3}He should also be lower than in pure liquid ^{4}He. Thus, as the ^{3}He concentration is increased and the equilibrium density of the mixture correspondingly smoothly decreases, the single-particle kinetic energies of both isotopes should monotonically decrease from their values in pure liquid ^{4}He to those in pure ^{3}He.

Experimental measurements [5] at $T = 1.4$ K have indeed shown such a decrease of the ^{4}He kinetic energy, from about 15 ± 3 K at $\chi = 0$ to 8 ± 3 K at $\chi = 0.4$; for ^{3}He, on the other hand, the kinetic energy is experimentally found to be 11 ± 3 K at all ^{3}He concentrations.

Our results for the kinetic energies of the two isotopes are summarized in Table I; for completeness, we have also included some results from Ref. [10]. A clear, monotonic dependence of the kinetic energy of *both* isotopes is observed in all finite systems studied. No extrapolation to the thermodynamic limit is needed to compare these results with experimental measurements, as finite-size corrections and statistical errors are much smaller than the reported experimental uncertainties. In Fig. 3 we compare our results for K_3 and K_4 for the 108-particle system with experimental results from Ref. [5]. Within experimental uncertainties, there is agreement between theory and experiment for ^{4}He, whereas for ^{3}He there is a statistically significant discrepancy between theory and experiment for χ at least up to 0.6.

In the light of the remarkable agreement with experiment obtained for the superfluid fraction as well as for other quantities, in the mixture [10] and in the pure liquids [8], it seems difficult to attribute the discrepancy either to PIMC or to the potential adopted. As for the possible

TABLE I. Single-particle kinetic energies $K_3(\chi, T)$ and $K_4(\chi, T)$ for ^{3}He and ^{4}He, computed by RPIMC at different ^{3}He concentrations χ and $T = 1$ and $T = 2$ K. N is the total number of particles in the system, and n is the number of ^{3}He particles (half for each spin projection). Statistical errors (in parentheses) are on the last digit. Stars mark results from Ref. [10].

N	n	χ	$T = 1$ K	$T = 2$ K	$T = 1$ K	$T = 2$ K
54	0	0.000			14.40(2)	15.41(5)
54	1	0.019	17.9(3)*		14.4(1)*	
54	6	0.111	17.65(3)	18.51(3)	13.80(1)	14.91(2)
54	10	0.185	17.42(3)		13.56(2)	
54	14	0.259	16.94(3)		13.26(2)	
54	18	0.333	16.77(1)	17.78(2)	12.78(1)	14.32(2)
54	26	0.481	16.28(1)		12.57(2)	
54	30	0.556	15.98(1)		12.38(2)	
54	34	0.630	15.77(2)		12.30(2)	
108	1	0.009	17.7(3)*	18.2(4)*	14.4(1)*	15.2(1)*
108	14	0.130	17.70(3)	18.49(2)	13.86(1)	15.12(2)
108	38	0.352	16.89(1)	17.60(2)	12.97(1)	14.32(1)
108	54	0.500	16.37(5)	16.76(2)	12.77(4)	13.63(2)
108	66	0.611	15.96(2)		12.38(4)	

effect of the fermion nodal restriction, we note that the disagreement with experiment is greatest in the $\chi \longrightarrow 0$ limit, i.e., where the restriction becomes unimportant, and the PIMC calculation is numerically exact.

Summarizing, we have carried out a RPIMC simulation of a homogeneous liquid helium mixture. Results for the ^{4}He superfluid fraction are in quantitative agreement with experiment; a significant discrepancy is instead reported between our results for the kinetic energy of ^{3}He and the values obtained in recent neutron scattering experiments.

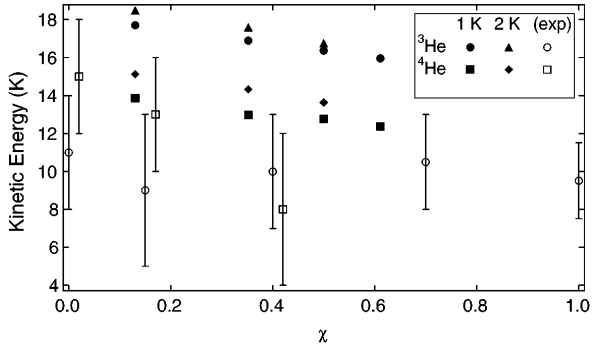

FIG. 3. Kinetic energies in a 108-particle isotopic liquid helium mixture, computed by RPIMC (filled symbols). Error bars are smaller than the size of the symbol. Also shown are experimental results (open symbols) from Ref. [5], obtained at $T = 1.4$ K.

This work was supported in part by the National Science Foundation under Research Grant DMR-9623961. The authors wish to acknowledge useful discussions with D. M. Ceperley, H. R. Glyde, G. Ortiz, and P. B. Weichman.

[1] J. Bardeen, G. Baym, and D. Pines, Phys. Rev. Lett. **17**, 372 (1966); M. Blume, V. J. Emery, and R. B. Griffiths, Phys. Rev. A **4**, 1071 (1971).
[2] See, for instance, G. Ahlers, in *The Physics of Liquid and Solid Helium*, Part I, edited by K. H. Benneman and J. B. Ketterson (Wiley, New York, 1976).
[3] S. B. Kim, J. Ma, and M. H. W. Chan, Phys. Rev. Lett. **71**, 2268 (1993).
[4] Y. Wang and P. E. Sokol, Phys. Rev. Lett. **72**, 1040 (1994).
[5] R. T. Azuah, W. G. Stirling, J. Mayers, I. F. Bailey, and P. E. Sokol, Phys. Rev. B **51**, 6780 (1995).
[6] W.-K. Lee and B. Goodman, Phys. Rev. B **24**, 2515 (1981); J. Boronat, A. Polls, and A. Fabrocini, J. Low Temp. Phys. **91**, 275(1993); N. Pavloff and J. Treiner, J. Low Temp. Phys. **83**, 331 (1991); E. Krotscheck and M. Saarela, Phys. Rep. **232**, 1 (1993).
[7] E. L. Pollock and D. M. Ceperley, Phys. Rev. B **36**, 8343 (1987).
[8] D. M. Ceperley, Rev. Mod. Phys. **67**, 279 (1995).
[9] E. L. Pollock and K. J. Runge, Phys. Rev. B **46**, 3535 (1992).
[10] M. Boninsegni and D. M. Ceperley, Phys. Rev. Lett. **74**, 2288 (1995).
[11] D. M. Ceperley, Phys. Rev. Lett. **69**, 331 (1992).
[12] E. C. Kerr, in *Proceedings of the Fifth International Conference on Low Temperature Physics and Chemistry*, edited by J. R. Dillinger (University of Wisconsin Press, 1958).
[13] R. A. Aziz, M. J. Slaman, A. Koide, A. R. Allnatt, and W. J. Meath, Mol. Phys. **77**, 321 (1992).
[14] D. M. Ceperley, J. Stat. Phys. **63**, 1237 (1991).
[15] V. I. Sobolev and B. N. Esel'son, Sov. Phys. JETP **33**, 132 (1971).
[16] See, for instance, M. N. Barber, in *Phase Transitions and Critical Phenomena*, edited by C. Domb and J. L. Lebowitz (Academic Press, New York, 1983), Vol. **8**.
[17] P. E. Sokol, T. R. Sosnick, and W. M. Snow, in *Momentum Distribution*, edited by R. N. Silver and P. E. Sokol (Plenum, New York, 1989); T. R. Sosnick, W. M. Snow, and P. E. Sokol, Phys. Rev. B **41**, 11 185 (1990).
[18] P. Whitlock and R. M. Panoff, Can. J. Phys. B **65**, 1409 (1987).